METRICA
METRology Institutional CAtalog

ISTITUTO NAZIONALE DI RICERCA METROLOGICA
Repository Istituzionale

Towards a new transfer standard for speed of sound measurements in liquids at cryogenic temperatures

This is the author's accepted version of the contribution published as:

Original
Towards a new transfer standard for speed of sound measurements in liquids at cryogenic temperatures / Cavuoto, G., Lago, S., Giuliano Albo, P.A.. - In: MEASUREMENT. - ISSN 0263-2241. - 180:(2021), pp. 1-8. [10.1016/j.measurement.2021.109526]

Availability:
This version is available at: 11696/70272 since: 2021-05-31T09:28:43Z

Publisher:
Elsevier

Published
DOI:10.1016/j.measurement.2021.109526

Terms of use:

This article is made available under terms and conditions as specified in the corresponding bibliographic description in the repository

Publisher copyright

(Article begins on next page)

01 July 2026

Towards a new transfer standard for speed of sound measurements in liquids at cryogenic temperatures

G. Cavuoto, S. Lago, P.A. Giuliano Albo

Istituto Nazionale di Ricerca Metrologica (INRiM), Strada delle Cacce 91, 10135 Torino, Italy

Abstract

Traceability of fluid flow measurement is a prerequisite for the accurate determination of transferred mass, heat and energy. However, considering the wide range of flow-rates, temperature, pressure, viscosity and densities, which is of interest for practical applications of fluid flow metrology, the accurate calibration of ultrasonic flow meters still represents a demanding task. Alternative to the usual gravimetric calibration, the possibility to provide traceability through using a speed of sound standard has been less explored. In this work, we describe and discuss the performance of an ultrasonic cell, and the feasibility of using this sensor to provide traceable measurements of the speed of sound. The instrument has been designed to serve as transfer standard for speed of sound and, its features make it suitable for the calibration of ultrasonic flowmeters both in the laboratory and on industrial pipelines. The sensor has been tested by performing speed of sound measurements in liquid methane between 100 K and 162 K and for pressure up to 10 MPa. The expanded relative uncertainty ($k = 2$) of the speed of sound w is $U_r(w) = 0.15\%$ for temperature below 130 K and $U_r(w) = 0.32\%$ above 130 K. The obtained results are found in agreement with previously published measurements and with the predictions of the Setzmann and Wagner and GERG equations of state. Along with the results of speed of sound measurements and their expanded ($k = 2$) uncertainty, we provide a detailed discussion of the procedures adopted to improve the stability of the sensor, and the specific corrections applied considering the cryogenic working conditions.

1. Introduction

Due to practical and cost limitations of calibration facilities, it is commonly accepted that flowmeters are calibrated in sub-ranges of flow, temperature and pressure, where very controlled conditions are possible. Even so, flowmeters can be operated over wider ranges by applying corrections, as reported in ISO 12242 standard [1]. The side effect of this disjunction is the possible manifestation of incoherent and misinterpreted on-site measurements that are amplified when the economic value of transferred fluid is high.

In the market of liquefied natural gas (LNG), flow meter calibration conditions are particularly difficult, due to the absence of facilities operating with pure methane, or LNG, at cryogenic conditions. At the moment, there are only a few facilities which are suitable for operation at cryogenic temperatures and, mainly, using liquid nitrogen [2,3]. In the near future, there will be the possibility to operate with LNG and the situation will improve but, even in this case, the calibration procedure will require stopping the line at the production site, to dismount and to deliver flowmeters, periodically. The complete stop of the industrial plant is usually prevented by creating a second measurement line that can operate when the first is under maintenance or calibration. This approach solves the problem of continuity, but does not eliminate possible effects caused by influencing quantities (i.e composition, temperature, pressure, heat flows, etc.), that can be different at the working site and at the calibration facility.

Ideally, calibrations should be performed on-site adopting transfer standards, when possible. This approach will allow to reduce costs, to eliminate the effects of influence quantities and it will give the possibility to verify sensors more often, in order to guarantee better performances of gauges over time.

Among available flowmeters types, ultrasonic sensors are promising the quickest evolution in terms of on-site calibration. Furthermore, they seem likely able to provide additional unexplored possibilities to obtain more information on the state of the flowing fluids. Some manufacturers are already supplying optional software for monitoring the profile of fluid speed with the aim to correct flow measurements.

Alternatively, combining the upstream and downstream times of flight of ultrasonic bursts, it is possible to separately determine the speed of the flowing mass and the speed of sound of the fluid, as it would be measured with the fluid at rest. The latter can be used to check the status of the fluid when compared with reference values. For example, in the case of binary mixtures, when accurate

models are available, it is possible to determine the fluid composition. Conversely, it is possible to verify the stability of the sensor in terms of calibration, when reference values are compared with those provided by gauges.

The ISO 12242 standard specifies requirements and recommendations for ultrasonic liquid flowmeters and states that sensors can perform self-tests without the need of repeated and costly full calibration services. The possibility to calibrate a ultrasonic flow meter using reference values of speed of sound is only briefly discussed in the ISO standard, probably because of a limited possibility of application of such an approach. As a matter of fact, reference speed of sound measurements are available only for a very limited number of fluids, many of them at purity grades not found on industrial plants. In this work we discuss the possibility to realize a transfer standard for speed of sound. Nowadays speed of sound measurements can be made traceable to the meter and the second [4-6] and sensor performance has been proven to be mainly independent of the measured fluids. As a first step, the traceability of a speed of sound measurement cell must be verified even when the sensor is calibrated at ambient conditions but measurements are performed at very different temperatures and pressures. This approach would allow to focus development efforts on the technological improvements of the transfer standard instead of on the many different classes of ultrasonic flowmeters. A calibrated speed of sound cell could be installed permanently, alongside ultrasonic flowmeters to provide needed reference values, at the same temperature, pressure and composition, whatever the flowing fluid is. The same transfer standard could be adopted for the calibration of temporary ultrasonic flowmeters (i.e. clamp-on) in the laboratory, where, thanks to provided reference values, it would be possible to determine almost all the parameters needed to calibrate the sensor without making use of independent propagation models of the sound in the removable supports where sources and receivers are set in (wedges).

2. Reference speed of sound measurements in liquid methane

The test fluid chosen in this work was methane because, being a pure substance, it can be easily reproduced at a know level of purity; it is the main component of LNG and thus both the speed of sound, the acoustic impedance and the signal wavelength are only slightly different from those of LNG. Furthermore, the scientific literature has many papers investigating thermodynamic properties of methane and, in particular, there are several works dedicated to speed of sound measurements [7-15].

Despite this, surprisingly, there are few studies focused on determining the speed of sound of methane at cryogenic temperatures. Specifically, since the second half of the 1960s until the end of the 1980s, only four works reported experimental results within the pressure range involved in the custody transfer process of LNG. These contributions [12-15] are listed in Table 1, where adopted experimental techniques, temperatures and pressures ranges and the declared uncertainties are listed.

Table 1. Previous published work discussing speed of sound measurements of methane at cryogenic temperatures.

Authors	Technique	T / K	p / MPa	Declared % uncertainty
Van Itterbeek, Thoen (1967)	Pulse superposition technique	111-190	0.1-18	0.1
Singer (1969)	Double pulse-echo	94-145	0.2-9	0.5
Straty (1974)	Pulsed technique	91-300	1.6-35	(0.05-0.2)
Baidakov (1982)	Pulsed technique	150-183	<4	(0.1-0.3)

The investigation of new on-line calibration approaches are particularly important in the field of LNG flow metering because of the economic value of the transferred fluid and the limited possibility to calibrate flowmeters at real operating conditions. For this reason a speed of sound measurement cell has been built and tested in a preliminary work [16] and obtained results showed that the performance is comparable with the best results available in literature, but they are still not sufficient to consider the sensor suitable as a transfer standard, in particular, at temperatures below 140 K, where the main problem was the limited repeatability of the measurements after several repeated temperature cycles from cryogenic to ambient conditions. The good agreement of the preliminary results, with those available in literature, and the successive analysis, that allowed to identify how the

expanded uncertainty of the measurement could be improved, inspired this work where the sensor performances are investigated extending the temperature range form 100 K to 160 K, in this way, the thermodynamic conditions found on industrial plants have been completely covered.

3. Measurement technique and corrections

Among several different possible measurement techniques [17], it has been chosen to approach the realization of a transfer standard by implementing the double pulse-echo method, since it is a well established, documented and already successfully adopted in different research contexts. In this technique, the measurement of the speed of sound is obtained by measuring the delay time between two acoustic signals, emitted simultaneously, traveling different path lengths at the same speed. Exhaustive descriptions of the measurement principle and its implementation can be found in [4,14,16-18] where also the main corrections to the measurements are described.

Speed of sound is calculated measuring the difference of the paths length $\Delta L = L_2 - L_1$ and the delay time τ as:

$$w_{\mathrm{exp}} = \frac{2\Delta L}{\tau + \delta\tau} \qquad (1)$$

where $\delta\tau$ is the correction to the delay time due to diffraction of the ultrasonic signals [17].

For a correct design of a sensor performing at cryogenic conditions, it is useful to take some precautions. For example, it is necessary to have an accurate model for the thermal expansion coefficient of the measurement cell and to avoid geometries for which the thermal stress can generate plastic deformations or failures of the sensor parts. Ultrasonic bursts are generated by a piezoelectric disk that is maintained in its position by a clamping system. Being particularly robust, and able to absorb the mechanical and thermal stresses, it has been chosen to adopt a polymer-encapsulated piezoelectric source, so that the piezoelectric would not crack if thermally stressed. In the course of our experimental tests, failures of the ultrasonic generation system have never been observed and calibration parameters of the sensor compared favorably even after tens of temperature cycles from ambient to cryogenic conditions.

After having evaluated different materials (ranging from grade 5 titanium to stainless invar) to build the measurement cell, the choice fell on AISI 316L stainless steel, because of its chemical stability, acoustic and mechanical properties. Preserving the cylindrical symmetry of the cell spacers, reflectors and the source support, corrections for temperature and pressure can be calculated with the necessary accuracy even for variations of hundreds kelvin and megapascal [18].

3.1. Temperature and pressure corrections

To compensate the effect of deformation occurring when temperatures and pressures are very different from those measured during calibration, the following differential equations have been used:

$$\left(\frac{\partial \Delta L(T,p)}{\partial T}\right)_p = \alpha(T)\Delta L(T,p) \qquad (2)$$

$$\left(\frac{\partial \Delta L(T,p)}{\partial p}\right)_T = \frac{\beta_T}{3}\Delta L(T,p) \qquad (3)$$

where β_T and α are the isothermal compressibility and the thermal expansion coefficient of the AISI-316L stainless steel, respectively. Performing measurements at cryogenic conditions, it is worth to consider, at least, the dependency of the thermal expansion coefficient of the AISI-316L stainless steel α on temperature and, hereafter, the expression suggested by NIST [19] for AISI-316L is adopted:

$$\alpha(T) = a + bT + cT^2 + dT^3, \qquad (4)$$

where T is temperature in kelvins, and the coefficients are $a = 5.867532 \cdot 10^{-7}$, $b = 1.405386 \cdot 10^{-7}\ \mathrm{K}^{-1}$, $c = 5.263604 \cdot 10^{-10}\ \mathrm{K}^{-2}$, $d = 7.604209 \cdot 10^{-7}\ \mathrm{K}^{-3}$.

Solving the differential equations in terms of ΔL the following expression is obtained:

$$\Delta L(T,p) = \Delta L(T_0,p_0)\left(1 + \alpha(T)\exp(\gamma) - \frac{\beta_T}{3}(p - p_0)\right), \qquad (5)$$

where $\Delta L(T_0,p_0)$ is the difference of paths length measured at calibration temperature T_0, and ambient pressure p_0, while $\gamma = a(T - T_0) + \frac{b}{2}(T^2 - T_0^2) + \frac{c}{3}(T^3 - T_0^3) + \frac{d}{4}(T^4 - T_0^4)$.

3.2. Temperature gradient corrections

Though, in laboratory conditions, temperature gradients can be controlled by two independent electric heaters, the same could not happen during on-site calibrations. In the case, the experimental time of flight $\tau_{\exp}$ can be corrected to minimize the effect of any residual temperature gradient which takes place in the direction of the acoustic path. The corrected delay time can be calculated, using the experimental delay time $\tau_{\exp}$ and the experimental value of speed of sound $w_{\exp}$, using the following expression:

$$\tau_g = \tau_{\exp}\left(1 + \frac{s}{\tau_{\exp} w_{\exp}^2}(L_2^2 - L_1^2)\right), \qquad (6)$$

where

$$s = \frac{\partial w}{\partial z} = \frac{\partial w}{\partial T}\frac{\partial T}{\partial z} \qquad (7)$$

is the sensitivity coefficient of the correction accounting for the variation of the speed of sound due to the temperature and the temperature gradient. In this expression, the coordinate z is the longitudinal axis of the measurement cell.

3.3. Diffraction corrections

The wave nature of the ultrasonic signals imposes further corrections to the delay time because received signals are not necessary in phase with each other due to the limited dimension of the source. Although, only an infinitely small or infinitely large source would generate perfectly phased signals, it is possible to design the measurement cell combining source diameter and acoustic paths length in a way that diffraction corrections remains small compared to other source of uncertainty [17].

In the same work the expressions for the corrections $\delta\tau$ are reported and they have been applied as it follows

$$\delta\tau = \frac{\phi(2L_2) - \phi(2L_1)}{\omega_0}, \qquad (8)$$

$$\phi(L) = \mathrm{Arg}\left[1 - \exp\left(-\frac{i2\omega_0 b^2/w_{\exp}}{2L}\right)\left(J_0\left(\frac{2\omega_0 b^2/w_{\exp}}{2L}\right) + iJ_1\left(\frac{2\omega_0 b^2/w_{\exp}}{2L}\right)\right)\right]. \qquad (9)$$

where $\omega_0 = 2\pi/f$, appearing in Eq. (8), is the pulsation of the carrier wave with the carrier frequency f, while the two terms $\phi(L)$ are the phase shifts, calculated as the functions of the length of the two spacers of the cell L_1 and L_2. Finally, the term b in Fig. 6 is the radius of the source, while J_0 and J_1 are Bessel functions of zero and first order, respectively.

Combining gradient and diffraction corrections, the actual delay time is calculated as:

$$\tilde{\tau} = \tau_g + \delta\tau \qquad (10)$$

while the corrected speed of sound $\tilde{w}$ is evaluated taking into account the corrected acoustic path length, by expression (5), and the corrected time of flight, by expression Eq. (8), as reported in the following equation.

$$\tilde{w} = \frac{2\Delta L(T,p)}{\tilde{\tau}}. \qquad (11)$$

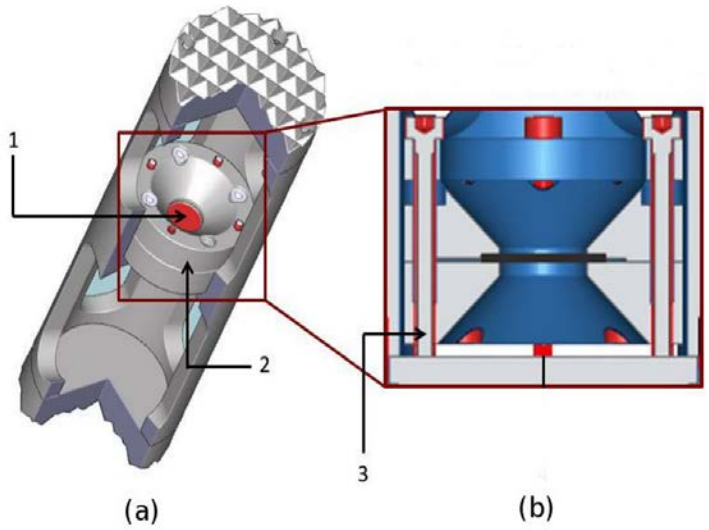

Fig. 1. *Ultrasonic cell (a) and longitudinal cross section (b) of the piezoelectric disk clamping system. (1) Piezoelectric disk. (2) Stainless steel clamping system. (3) Steel screw to secure the locking system to the ultrasonic cell.*

4. Experimental apparatus for cryogenic speed of sound measurements

The core element of the apparatus is a 75 mm long ultrasonic cell made of stainless steel AISI 316L, which includes two spacers of different nominal lengths: $L_1 = 45$ mm and $L_2 = 30$ mm. As depicted in Fig. 1, the ultrasonic source, which is a piezo-electric disk with an active diameter of 7 mm, is clamped by the support using four screws, in gray color in the picture. The measuring cell is housed in a control system for temperature and pressure namely the cryostat and the pressure vessel.

To properly perform in the range of 100 K and 160 K, a dedicated temperature control system has been designed to compensate for unwanted heat fluxes from the ambient in the form of radiation (typically small, but measurable) and conduction (the main contribution). The operation and elements that make up this thermal control unit have been described in detail in a previous work [16]. In the same work, a deep description of the thermal unit and the control system has been reported, thus only a brief description is given here.

The sensor is attached on the upper flange of the AISI 316L pressure vessel, that is able to operate up to 70 MPa while the system cooling is provided by liquid nitrogen which flows into an aluminum cylindrical heat exchanger.

Though this temperature control unit is much simpler than those adopted for traditional cryostats, the achieved temperature stability was better than ± 25 mK and the temperature gradient from the top to the bottom of the pressure vessel never exceeded 80 mK, in the worst case.

The ultrasonic transducer was excited by a function generator with a 10-cycle sinusoidal tone-burst characterized by a carrier frequency of 4 MHz and an peak-to-peak amplitude of 10 V.

Table 2. List of the expanded uncertainty sources for the calculation of the overall uncertainty (with $k = 2$) of speed of sound for temperatures above 130 K and below 130 K.

Uncertainty source	Contribution / %	Distribution
Temperature above 130 K		
Acoustic path length	0.030	Normal
Time of flight	0.004	Normal
Temperature	0.116	Rectangular
Pressure	0.104	Rectangular
Repeatability	0.036	Normal
Relative expanded combined uncertainty ($k = 2$)	<0.32	
Temperature below 130 K		

Uncertainty source	Contribution / %	Distribution
Acoustic path length	0.030	Normal
Time of flight	0.004	Normal
Temperature	0.056	Rectangular
Pressure	0.0282	Rectangular
Repeatability	0.036	Normal
Relative expanded combined uncertainty ($k = 2$)	<0.15	

The traceability of the speed of sound measurements is guaranteed by the calibration certificates of the thermometers, the pressure transducer, the time-base of the oscilloscope and of the cell paths lengths.

In particular, the temperature of measuring cell was obtained as the mean value of the resistances measured by two PT100 thermometers placed inside the walls of the pressure vessel. These sensors were calibrated by using the international temperature scale ITS-90 [20], using fixed points from argon to gallium, with a expanded uncertainty of ± 0.02 K. The pressure of the liquid methane was measured by a temperature controlled pressure transducer (Honeywell Super TJE) placed on the inlet line of methane and calibrated with an expanded uncertainty of ± 0.025 MPa, up to 50 MPa.

5. Ultrasonic cell improvement

In the work [16], materials and measurement procedures were tested for temperature between 130 K and 162 K and pressure up to 10 MPa. Results showed deviations of up to 1.5% from the values predicted by the equation of state for temperatures below 140 K. Moreover, at lower temperatures, the experimental results were not consistent with speed of sound values available in literature and the repeatability was poor. For these reasons, the performance of the cell was verified alternating cryogenic temperature cycles and cell calibration using water as a reference fluid. Usually the repeatability of the calibration was better than 50 parts per million (ppm) of the acoustic path lengths, however, in this case it was 50 times worse and degraded after each temperature cycle. Since, during thermal cycles, the most thermally stressed parts of the sensor were the screws used to fix the ultrasonic source, it was decided to substitute them but without success. After some trials, it was found that the problem could be solved by reducing the length of those screws.

The piezoelectric disk was in fact mounted inside the measuring cell through a clamping system consisting of two AISI 316L stainless steel supports, screwed together firstly, and then fastened to the cell as shown in Fig. 1(B). A careful check showed that their length was such that, after a few measurement cycles, they were plastically deformed and extended, after reaching the room temperature again. After being deformed, they pushed against the support of the cell used to fix the piezoelectric. The resulting effect was that the relative position of the acoustic source, with respect to the reflective walls of the cell, changed from time to time, becoming sensitive to the temperature excursion and the number of thermal cycles. These changes resulted in an enhancement of the repeatability which has been improved to better than 0.05%, therefore in the order of magnitude expected for a cell working at ambient temperature.

Furthermore, it was observed that the disassembly operations of the shortened screws of the cell undergone plastic deformations. As a matter of fact, though the repeatability of the measurements was better than 500 ppm, also after tens of thermal cycles, when dismounted and remounted, the repeatability of the successive measurements become 5 times worse, when using the same screws.

For this reason, re-calibration of the cell is strictly necessary every time the screws have been removed and substituted while, in other cases, the cell can support tens of thermals cycles without showing degrading performances. Purely by way of example, Fig. 2 shows the results of two repeated measurements at 110 K, when screws have been replaced and the cell has been re-calibrated. The agreement was better that 0.04% and probably perturbed by different stability conditions of the measurement system. As a matter of fact, when mounting problems had occurred the repeatability would be an order of magnitude worse, at least.

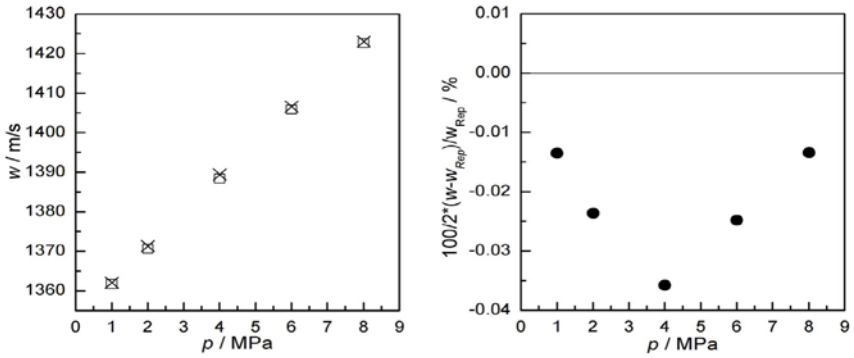

Fig. 2. *Left plot shows absolute speed of sound measured at 110 K for pressures up to 8 MPa. (□) First measurement at 110 K; (×) repeated measurement. Right plot shows the relative deviations of the repeated measurements.*

6. Ultrasonic cell calibration

In this work, where the feasibility of the realization of a standard of transfer for speed of sound is investigated, it has been decided to calibrate the cell using pure water at ambient temperature and to reserve an absolute calibration, traceable to standard of length and time, only at the end of the measurements if the mechanical stability of the cell was confirmed. Since the measurements were carried out at temperatures far below those at which the cell was calibrated, the contribution of the uncertainty affecting the thermal expansion coefficient has been explicitly reported. In this case, it has been used the thermal expansion coefficients of AISI-316L stainless steel, reported in [19] and derived from experimental measurements, described in the work of Beenakker and Swenson [21], which have an estimated experimental uncertainty $u(\alpha) = \pm 3 \times 10^{-5}\ \mathrm{K}^{-1}$. Having calibrated the path lengths of the speed of sound sensor using a reference fluid, the relative standard uncertainty associated to the acoustic path determination, $\sigma(\Delta L)/\Delta L$, is calculated as follows:

$$\frac{u(\Delta L)}{\Delta L} = \sqrt{\left(\frac{u(w_w)}{w_w}\right)^2 + \left(\frac{u(\tau)}{\tau}\right)^2 + \left(\frac{u(T_0)}{w_w}\frac{\partial w_w}{\partial T_0}\right)^2 + \left(\frac{u(p_0)}{w_w}\frac{\partial w_w}{\partial p_0}\right)^2 + \left(\Delta T\, u(\alpha)\right)^2}, \qquad (12)$$

where $\Delta T = 194$ K has been calculated in the worst case while w_w is the speed of sound in water, at ambient temperature, T_0, and at atmospheric pressure, p_0, obtained from the IAPWS-95 formulation [22] and used as reference values. The relative uncertainty of the length measurement obtained by calibration using the speed of sound in pure water was estimated to be approximately 300 ppm and expression (12) allowed to easily check if successive calibrations of the cell are consistent.

In a different frame of the present work, where the speed of sound measurements were made fully traceable, the acoustic path length would have been measured using a coordinate measurement machine (CMM) as it had been already done in [4] where absolute speed of sound measurements had been performed. It is worth to notice that CMM measurements may not provide the best uncertainty, but they would preserve the traceability chain. As a matter of fact, in the case of speed of sound cells, the limits in the mechanical realization of the sensor have a significant impact on the accuracy of the measurements. While the measuring system operates with typical standard uncertainties below 0.5 μm ($k = 2$), errors in parallelism and flatness of source and reflector surfaces would contribute to increase the uncertainty up to 2 μm. In this way the uncertainty affecting the difference of path lengths would be in the order of 0.004 mm, that would lead to a relative standard uncertainty in the order of 0.03%. A relative calibrations made using a reference materials (i.e. argon, helium, etc.) might provide a better uncertainty, but the traceability of the calibration should have been proven considering how the material has been characterized including the possibility that a different composition of reference material may have an impact.

7. Uncertainty analysis

Since the speed of sound $w(T,p)$ is obtained by the independent determination of both the difference of the acoustic paths lengths ΔL, and the delay time τ, and through the measurements of the temperatures T, and the pressures p, at which the measurements have been carried out, it is possible to estimate its standard uncertainty by using the following expression for error propagation:

$$\frac{\sigma(w)}{w} = \sqrt{\left(\frac{\sigma(\Delta L)}{\Delta L}\right)^2 + \left(\frac{\sigma(\tau)}{\tau}\right)^2 + \left(\frac{\sigma(T)}{w}\frac{\partial w}{\partial T}\right)^2 + \left(\frac{\sigma(p)}{w}\frac{\partial w}{\partial p}\right)^2 + R^2}, \qquad (13)$$

where R is the relative repeatability of the measurements.

The uncertainty associated with time of flight $\sigma(\tau)$ has been demonstrated to be twice the oscilloscope sampling interval [4]; while the temperature uncertainty, namely the uncertainty of the platinum resistance thermometers (PT100) used in this experiment, is 0.02 K. The pressure uncertainty is 0.025 MPa and, finally, the temperature and pressure dependency terms, $\partial w/\partial T$ and $\partial w/\partial p$, are obtained by fitting the experimental results. Table 2 reports the main contributions, including the scaling effects of sensitivity coefficients, to the standard uncertainty of the experimental measurements of speed of sound.

The sensitivity coefficients have been approximated considering the worst condition over specific pressure or temperature intervals. Since it has been observed a factor of two between coefficients below and above 130 K, it has been decided to split the expanded uncertainty budget so that between 100 K and 130 K, the range of interest for industrial purposes, the uncertainty is not overestimated too much.

The repeatability R is estimated to be better than 0.036% though this value has been observed only once and it is usually much better. Anyway, this contribution to the expanded uncertainty budget is much smaller than others and, reducing it by a factor of two produces an improvement of the expanded uncertainty of only 0.01%.

Finally, the expanded relative uncertainty in speed of sound, with a coverage factor $k = 2$, has been estimated to not exceed 0.32%, for temperatures above 130 K and 0.15%, for temperatures below 130 K.

Table 3. Purity characterization of the methane adopted in this work.

Chemical name	Source	Initial Mole Fraction Purity	Purification Method	Final Mole Fraction Purity	Analysis Method
Methane (CAS no.: 74-82-8)	SIAD, ITALY	0.999995	none	-	-

Table 4. Experimental values of speed of sound in liquid methane. The uncertainty associated to temperature measurements is $u(T) = 0.02$ K; that of pressure is $u(p) = 0.025$ MPa and the expanded relative combined uncertainty for speed of sound is $U_r(w) = 0.15\%$ ($k = 2$) for temperatures below 140 K and $U_r(w) = 0.32\%$ ($k = 2$) for higher temperatures.

T / K	***p* / MPa**	***ω* / m s^{-1}**	**T / K**	***p* / MPa**	***ω* / m s^{-1}**
100.10	0.950	1458.9	140.01	2.055	1058.6
100.09	2.104	1468.3	140.01	4.079	1089.8
100.08	4.047	1483.4	140.03	6.228	1120.2
100.09	6.046	1498.3	140.10	8.044	1143.5
100.11	8.013	1512.4	140.06	9.967	1168.0
100.18	10.064	1526.2			
110.03	1.026	1362.0	150.13	2.073	939.4
110.02	2.024	1371.4	150.15	4.028	977.6
109.95	3.987	1389.8	150.09	5.939	1012
109.99	6.124	1407.8	150.08	8.093	1046.9
110.06	8.100	1423.4	150.10	10.137	1077.5
110.02	9.981	1438.7			

T / K	p / MPa	ω / m s^{-1}	T / K	p / MPa	ω / m s^{-1}
120.01	1.079	1261.4	161.85	1.951	776.3
120.02	2.052	1271.7	162.01	4.104	835.9
120.02	4.036	1292.6	162.00	6.035	882.0
120.00	6.019	1312.5	161.97	8.089	925.1
120.07	7.983	1331	161.98	9.925	959.4
120.02	10.099	1351.2			
130.03	2.058	1167.7			
130.01	4.043	1193.3			
129.94	5.983	1216.7			
129.99	8.059	1239.8			
130.03	10.007	1260.3			

8. Results and comments

The sample of gaseous methane was provided by SIAD and stored in a 50 liter cylinder. According to the supplier's certification, reported in Table 3, the gas was pure at the 99.9995% mol and no further purification process was done.

The speed of sound has been measured along seven isotherms (100, 110, 120, 130, 140, 150, 162) K and for pressures up to 10 MPa.

For safety reasons, the pressure vessel was evacuated and cooled down to a temperature of approximately 15 K below the measurement set point. In this way, the gaseous methane, injected at ambient temperature, heated the system up to a temperature closed to that one established for the measurement.

Table 5. Available literature values of speed of sound in liquid methane for T between (100 and 160) K and for pressure up to 10 MPa.

Author	T / K	p / MPa	ω / m s^{-1}	$u_r(w)\cdot 10^2$	Author	T / K	p / MPa	ω / m s^{-1}	$u_r(w)\cdot 10^2$
Van Itterbeek et al. [12]	125.1	1.0102	1209	0.1	Singer [13]	145.6	8.5808	1100	0.5
	125.1	1.991	1220.8	0.1		145.6	1.824	980	0.5
	125.1	3.9172	1242.7	0.1		124.9	5.884	1260	0.5
	125.1	5.9235	1265.1	0.1		125.1	1.0199	1210	0.5
	125.1	8.7747	1295	0.1		125	7.9434	1282	0.5
	125.1	9.788	1305.2	0.1		125	3.5402	1240	0.5
	111.33	0.9808	1349.6	0.1		125.1	8.7377	1295	0.5
	111.33	1.9728	1358.7	0.1		112	8.7279	1430	0.5
	111.33	3.9324	1376.6	0.1		112.1	6.1292	1400	0.5
	111.33	5.8839	1393.1	0.1	Straty [14]	120	9.258	1345.2	0.2
	111.33	7.569	1408.5	0.1		120	4.367	1290.5	0.2
	140.03	1.988	1059.5	0.1		100	1.661	1465.1	0.2
	140.03	3.9344	1089.1	0.1		100	7.244	1507.4	0.2
	140.03	5.8991	1117.9	0.1		150	7.263	1036.6	0.2
	140.03	7.8932	1145.3	0.1		150	3.02	962.1	0.2

Author	T / K	p / MPa	ω / m s^{-1}	$u_r(w)\cdot10^2$	Author	T / K	p / MPa	ω / m s^{-1}	$u_r(w)\cdot10^2$
	140.03	9.788	1169.5	0.1	Baidakov [15] et al.	150	4.001	980.7	0.2
	155.43	2.1451	872.9	0.1		150	2.045	942.1	0.3
	155.43	3.9811	915.1	0.1		160	3.998	861.2	0.3
	155.43	5.9295	954.5	0.1		160	2.043	809	0.3
	155.43	7.8426	990.5	0.1					
	155.43	9.7779	1022.5	0.1					

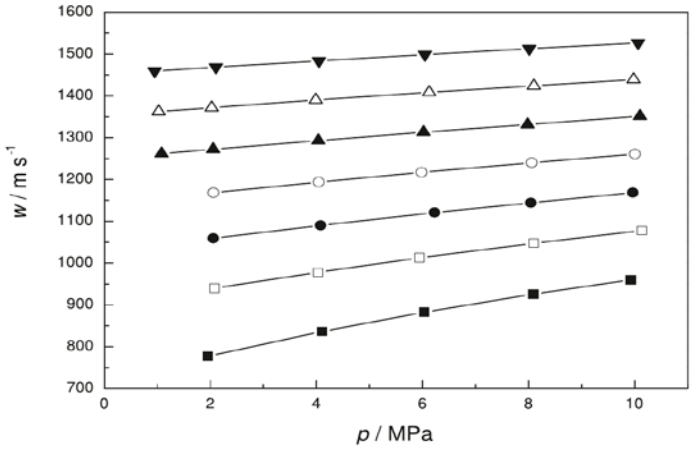

Fig. 3. *Experimental speeds of sound in liquid methane measured in this work as a function of pressure at different temperatures. (▾) $T = 100$ K; (▵) $T = 110$ K; (▴) $T = 120$ K; (○) $T = 130$ K; (●) $T = 140$ K; (□) $T = 150$ K; (■) $T = 162$ K.*

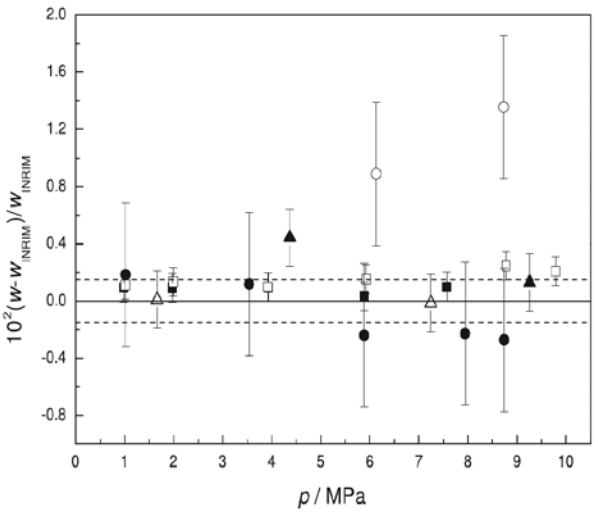

Fig. 4. *Comparison between experimental speed of sound with those available in literature for temperature below 130 K. (■) Van Itterbeek et al. $T = 111$ K; (□) Van Itterbeek et al. $T = 125$ K; (○) Singer, $T = 112$ K; (●) Singer, $T = 125$ K; (▵) Straty, $T = 100$ K; (▴) Straty, $T = 120$ K. The expanded uncertainty of INRiM speed of sound values is $U_r(w) = 0.15\%$ with a coverage factor $k = 2$.*

Collected experimental speeds of sound, as reported in Table 4 and plotted in Fig. 3, have been compared with the results available in literature, specifically, with the results of the works listed in Table 1. For the sake of completeness, literature results are reported in Table 5 with the corresponding uncertainty values. The relative deviations are reported in plot 4, for temperature below 130 K, and in plot 5, for temperature above 130 K. The experimental speeds of sound, w_{INRiM}, have been compared with the measurements available in literature, provided at the corresponding temperatures T_{lit} and pressures p_{lit}, accounting for small differences of temperature and pressure by the expression:

$$w_c = w_{\mathrm{INRiM}} + \left(\frac{\partial w}{\partial T}\right)_p (T_{\mathrm{lit}} - T_{\mathrm{INRiM}}) + \left(\frac{\partial w}{\partial p}\right)_T (p_{\mathrm{lit}} - p_{\mathrm{INRiM}}), \qquad (14)$$

where w_c is the corrected value and both terms $\partial w/\partial T$ and $\partial w/\partial p$ were calculated empirically for each (T, p) point by a 2nd-order polynomial fit.

Comparison of lower temperature results shows that, with few exception, the literature results are compatible even not including the uncertainty of the present values. In very few other cases, measurements are in agreement within the combined uncertainties, and only one of the measurements of Straty at 120 K, and two of Singer at 110 K, are not compatible.

Particular attention should be placed on the agreement between the new measures and the results obtained by Van Itterbeek et al. In fact, in [16], there was a lack of consistency between the speeds of sound measured at lower temperatures ($T < 130$ K) and the expected values, that new measurements have resolved.

Similarly, as plotted in Fig. 5, the comparison for temperatures above 130 K shows that the new experimental speeds of sound are all in agreement, within the combined uncertainties, with the results found in literature. The only exception is a single point provided by Singer. In this range of temperature, the agreement with the results reported by Van Itterbeek et al. is of particular interest, as the previous measurements disagreed, at $T = 145$ K and at $T = 150$ K, up to 0.8% at the lowest pressures [16].

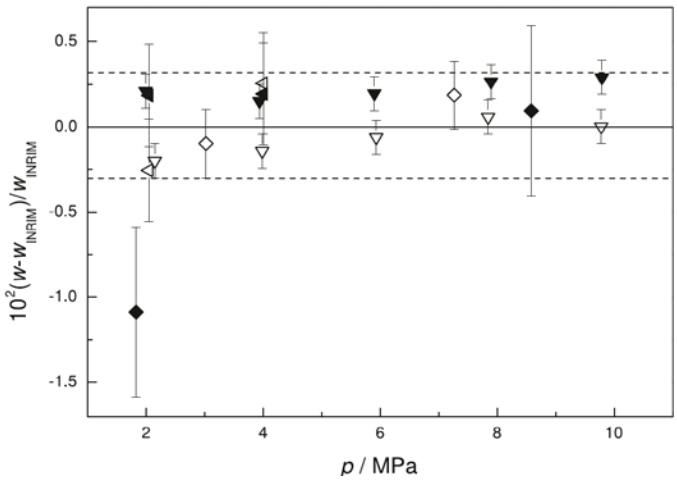

Fig. 5. *Comparison between experimental speed of sound and those available in literature for temperature above 130 K. (▾) Van Itterbeek et al. $T = 140$ K; (▿) Van Itterbeek et al. $T = 155$ K; (◆) Singer, $T = 145$ K; (◇) Straty, $T = 150$ K; (filled left triangle) Baidakov et al. $T = 150$ K; (open left triangle) Baidakov et al. $T = 160$ K. The expanded uncertainty of INRiM speed of sound measurements is $U_r(w) = 0.32\%$ ($k = 2$).*

The noticeable improvement in the agreement with Van Itterbeek's measurements is another evidence of how the changes implemented in the measuring cell have led to an improvement in the stability of the measurements at lower temperatures.

In addition to the data available in literature, the experimental results have been also compared with the speed of sound values predicted by two formulations: the fundamental equation of state of methane by Setzmann and Wagner [23] and GERG-2008 [24]. The results of these comparisons are plotted in Figs. 6 and 7, respectively. The Setzmann and Wagner's equation of state has an estimated uncertainty for speed of sound that varies from 0.15%, for temperatures above 150 K, to 0.3% at lower temperatures. In the same way, the uncertainty of GERG-2008 formulation ranges from 0.5%, above 150 K, to 1% at lower temperatures. Considering the uncertainties of the equations of state and the expanded uncertainty ($k = 2$) associated with the experimental measurements, it can be seen that all the speeds of sound value obtained in this work are in agreement with predictions of both the formulations.

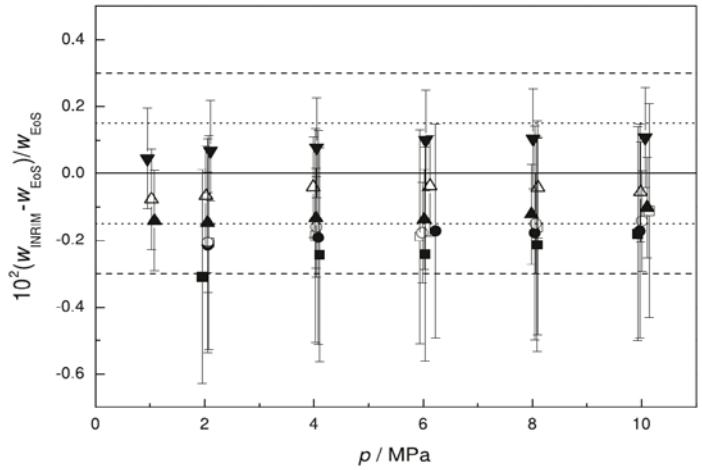

Fig. 6. *Comparison between experimental speed of sound and those predicted by the Setzmann and Wagner equation of state. (▾) $T = 100$ K; (▵) $T = 110$ K; (▴) $T = 120$ K; (○) $T = 130$ K; (●) $T = 140$ K; (□) $T = 150$ K; (■) $T = 162$ K. Dotted horizontal lines represents the speed of sound uncertainty of Setzmann and Wagner formulation, $u(w) = 0.15\%$ for $T > 150$ K. Dashed horizontal lines shows speed of sound uncertainty of Setzmann and Wagner formulation, $u(w) = 0.30\%$ for $T < 150$ K. The expanded relative uncertainty of INRiM measurement is $U_r(w) = 0.32\%$ for $T > 130$ K and $U_r(w) = 0.15\%$ for $T < 130$ K with a coverage factor $k = 2$.*

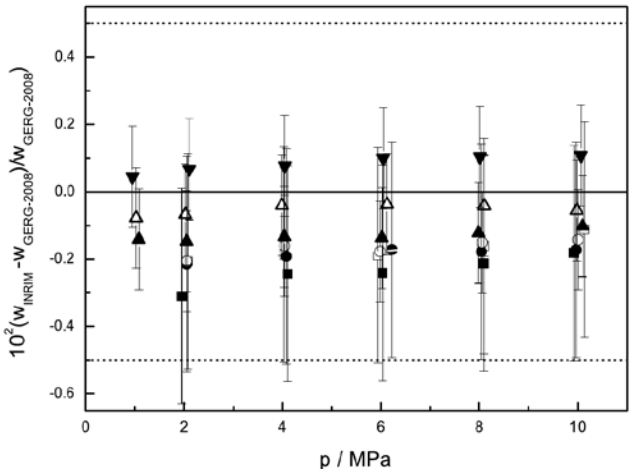

Fig. 7. *Comparison between experimental speed of sound and those predicted by the GERG-2008 formulation. (▾) $T = 100$ K; (▵) $T = 110$ K; (▴) $T = 120$ K; (○) $T = 130$ K; (●) $T = 140$ K; (□) $T = 150$ K; (■) $T = 162$ K. Dotted horizontal lines represents speed of sound uncertainty of GERG-2008 equation of state, $u(w) = 0.5\%$ for $T > 150$ K while the uncertainty is $u(w) = 1\%$ for $T < 150$ K. INRiM results have an expanded uncertainty $U_r(w) = 0.32\%$ for $T > 130$ K and $U_r(w) = 0.15\%$ for $T < 130$ K, with a coverage factor $k = 2$.*

The largest deviations occur for measurements at 162 K, especially at lower pressures, where the measurements deviate from the predictions of the mathematical models between (0.3 and 0.4)%. Despite this, even these results are largely within the declared uncertainty.

Though further improvements of the performances of the measurement cell will not be achieved in next few years, the actual measurement capabilities already allow to start exploring the new applications derived by availability of a feasible traceable transfer standard for speed of sound measurements.

After laboratory calibration, the cell could be housed in a 2''-DN50 tee-spool as reported in Fig. 8. In this way, the cell would not perturb the main flow and it could provide reference values of speed of sound, as the fluid was at rest. Obtained results could be compared with those measured by each path of a permanently installed ultrasonic flow meter and used to calibrate each acoustic paths. Furthermore, including a couple of valves, the installation of the transfer standard would not request to stop the main flow.

9. Conclusions

The aim of this work was to demonstrate, with experimental measurements, the possibility to develop a transfer standard for speed of sound measurement to be used as possible alternative method for the calibration of ultrasonic flowmeters. A transfer standard would allow both to verify, on-site, the stability of gauges and to open up the opportunity to use the speed of sound measured values for a traceable monitoring the quality of the transferred fluid.

The laboratory experimental apparatus used for the speed of sound measurement has been characterized in the temperature range between (100 and 162) K and for pressures from (1 to 10) MPa and it has been demonstrated that fully traceable experimental speed of sound are possible at cryogenic conditions also.

These experiments allowed to identify and to resolve the imperfections of the measurement cell as proved by the increased repeatability and the better expanded relative uncertainty, being reduced from 0.42% of [16] to 0.15% of this work.

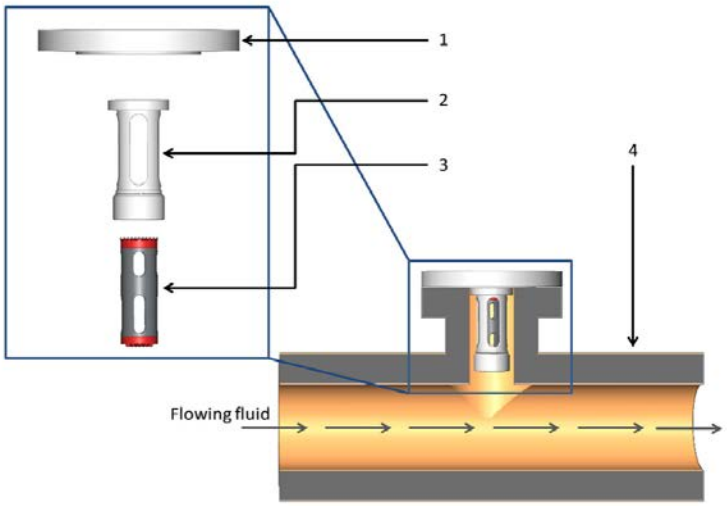

Fig. 8. *Scheme which shows how the ultrasonic cell can be used as a transfer standard by mounting it directly on the pipelines where LNGs flow, in vicinity of the ultrasonic flowmeters to be calibrated. (1) DN 50 flange; (2) Stainless steel support for the ultrasonic cell; (3) Ultrasonic cell; (4) LNG pipeline T-connection.*

Acknowledgments

This project (16ENG09-LNG3) has received funding from the EMPIR programme co-financed by the Participating States and from the European Union's Horizon 2020 research and innovation programme.

The authors are grateful to all who have contributed to this work, especially to Marco Bertinetti for his valuable help in designing and manufacturing new components of the experimental apparatus. A special thanks also goes to Emanuele Audrito, Elio Keith Bertacco and Stefano Pavarelli for having ensured the regular supply of liquid nitrogen.

Appendix A. Supplementary data

Supplementary material related to this article can be found online at https://doi.org/10.1016/j.measurement.2021.109526.

References

[1] ISO Standard 12242, in: Measurement of Fluid Flow in Closed Conducts-Ultrasonic Transit-Time Meter for Liquid, 2012.

[2] M. Van der Beek, P. Lucas, O. Kerkhof, M. Mirzaei, G. Blom, Results of the evaluation and preliminary validation of a primary LNG mass flow standard, Metrologia 51 (5) (2014) 539.

[3] T. Kegel, The NIST/CEESI liquid nitrogen flow facility, in: European Flow Measurement Workshop, Metrology for LNG, CEESI European Flow Measurement Workshop, 2017.

[4] G. Benedetto, R.M. Gavioso, P.A. Giuliano Albo, S. Lago, D. Madonna Ripa, R. Spagnolo, Speed of sound in pure water at temperatures between 274 K and 394 K and at pressures up to 90 MPa, Int. J. Thermophys. 26 (6) (2005) 1667-1680.

[5] K.I. Fujii, R. Masui, Accurate measurements of the sound velocity in pure water by combining a coherent phase-detection technique and a variable path-length interferometer, J. Acoust. Soc. Am. 93 (1) (1993) 276-282.

[6] V.A. Del Grosso, C.W. Mader, Speed of sound in pure water, J. Acoust. Soc. Am. 52 (5B) (1972) 1442-1446.

[7] H.B. Dixon, C. Campbell, A. Parker, On the velocity of sound in gases at high temperatures and the ratio of the specific heats, Proc. R. Soc A 100 (702) (1921) 1-26.

[8] A. Van Itterbeek, L. Verhaegen, Measurements of the velocity of sound in liquid Argon and liquid Methane, Proc. Math. Phys. Soc. B 62 (1949) 800.

[9] W. Van Dael, A. Van Itterbeek, J. Thoen, A. Cops, Sound velocity measurements in liquid Methane, Physica 31 (11) (1965) 1643-1648.

[10] Yu P. Balgoi, A.E. Buko, S.A. Mikhailenko, V.V. Yakuba, Velocity of sound in liquid Kripton, Xenon and Methane, Russ. J. Phys. Chem. 41 (7) (1967) 908.

[11] B.E. Gammon, D.R. Douslin, The velocity of sound and heat capacity in methane from nearcritical to subcritical conditions and equation of state implications, J. Chem. Phys. 64 (1) (1976) 203.

[12] A. Van Itterbeek, J. Thoen, A. Cops, W. Van Dael, Sound velocity measurements in liquid methane as a function of pressure, Physica 35 (1) (1967) 162-166.

[13] J.R. Singer, Excess ultrasonic attenuation and volume viscosity in liquid methane, J. Chem. Phys. 51 (11) (1969) 4729-4733.

[14] G.C. Straty, Hypersonic velocities in saturated and compressed fluid methane, Cryogenics 15 (12) (1975) 729-731.

[15] V.G. Baidakov, A.M. Kaverin, Measurement of ultrasonic speed in stable and metastable liquid methane, J. Chem. Thermodyn. 14 (11) (1982) 1003-1010.

[16] G. Cavuoto, S. Lago, P.A.G. Albo, D. Serazio, Speed of sound measurements in liquid methane (CH4) at cryogenic temperatures between (130 and 162) K and at pressures up to 10 MPa, J. Chem. Thermodyn. 142 (2020) 106007.

[17] J.P.M. Trusler, Physical Acoustics and Metrology of Fluids, Adam Hilger, Bristol, 1991.

[18] C.W. Lin, J.P.M. Trusler, The speed of sound and derived thermodynamic properties of pure water at temperatures between (253 and 473) K and at pressures up to 400 MPa, J. Chem. Phys. 136 (9) (2012) 094511.

[19] R.J. Corruccini, J.J. Gniewck, Thermal Expansion of Technical Solids at Low Temperatures: A Compilation from the Literature, National Bureau of Standards, vol. 29, US Department of Commerce, National Bureau of Standards, US. Gov. Printing Office 24, Washington DC, 1961.

[20] H. Preston-Thomas, The international temperature scale of 1990 (ITS90), Metrologia 27 (1990) 3-10.

[21] J.J.M. Beenakker, C.A. Swenson, Total thermal contractions of some technical metals to 4.2° K, Rev. Sci. Instrum. 26.12 (1955) 1204-1205.

[22] W. Wagner, A. Pruss, The IAPWS formulation 1995 for the thermodynamic properties of ordinary water substance for general and scientific use, J. Phys. Chem. Ref. Data 31 (2) (2002) 387-535.

[23] U. Setzmann, W. Wagner, A new equation of state and tables of thermodynamic properties for Methane covering the range from the melting line to 625 K at pressures up to 1000 MPa, J. Phys. Chem. Ref. Data 20 (6) (1991) 1061-1155.

[24] O. Kunz, W. Wagner, The GERG-2008 wide-range equation of state for natural gases and other mixtures: An expansion of GERG-2004, J. Chem. Eng. Data 57 (11) (2012) 3032-3091.